J|A|C|S
ARTICLES
Published on Web 12/22/2005

Rapid Access to Unexplored Chemical Space by Ligand Scanning around a Ruthenium Center: Discovery of Potent and Selective Protein Kinase Inhibitors

Howard Bregman, Patrick J. Carroll, and Eric Meggers*

Contribution from the Department of Chemistry, University of Pennsylvania, 231 South 34th Street, Philadelphia, Pennsylvania 19104

Received August 21, 2005; E-mail: meggers@sas.upenn.edu

Abstract: An important objective for the discovery of compounds with unique biological activities is the development of methods for the synthesis of molecular scaffolds with defined three-dimensional shapes. We are currently investigating the scope of using metal complexes to accomplish this goal. In these compounds, the metal center has the role of organizing the orientation of the organic ligands, thus defining the overall shape of the molecule. A strategy is presented that allows a rapid scanning of ligands around a ruthenium center in the search for ligand spheres that are complementary in shape and functional group presentation to ATP binding sites of protein kinases. Following this approach, we have identified octahedral ruthenium complexes as potent inhibitors for the protein kinases Pim1, MSK1, and GSK3α.

Introduction

Natural products display a high diversity of molecular skeleta, and many complex natural products adopt very distinctive three-dimensional conformations.[1] Unquestionably, these defined structures are important for their unique biological properties. As a consequence, an important challenge for the future discovery of synthetic molecular probes with superior biological properties is the development of methods for the economical synthesis of molecules with defined three-dimensional shapes.[2,3]

We recently started a program that aims in exploring small molecule chemical space with metal-containing compounds.[4−9] In these molecules, the coordinative bonds are designed to be kinetically inert and thus stable in biological environments. Hence, such metal complexes are supposed to behave like purely organic compounds without displaying any metal-related cytotoxicities.[6] We believe that the addition of a metal to an otherwise organic scaffold opens new opportunities for the design of bioactive molecules with novel properties.[7−9] First, it gives access to areas of the chemical space that may not be easily accessible with purely organic scaffolds. In this respect, we like to think of a chemically inert metal center as a "hypervalent carbon" with extended structural opportunities. Second, metal complexes are built from a central core and thus may have an advantage in building shape and functional group diversity in an economical fashion. We here demonstrate the power of this strategy with the discovery of novel octahedral ruthenium complexes as potent protein kinase inhibitors, all synthesized from a common precursor complex by a rapid ligand scanning protocol.

Our strategy for the design of metal complexes as protein kinase inhibitors uses the indolocarbazole alkaloid staurosporine as a lead structure (Figure 1).[10] Staurosporine adopts a very defined globular structure with the carbohydrate moiety being oriented perpendicular to the plane of the indolocarbazole heterocycle. The indolo[2,3-*a*]carbazole moiety occupies the hydrophobic adenine binding cleft, with the lactam group mimicking the hydrogen bonding pattern of the adenine base by usually forming two canonical hydrogen bonds to the backbone of the hinge between the N-terminal and C-terminal domains.[11] The carbohydrate moiety forms hydrophobic contacts

(1) (a) Newman, D. J.; Cragg, G. M.; Snader, K. M. *Nat. Prod. Rep.* **2000**, *17*, 215−234. (b) Clardey, J.; Walsh, C. *Nature* **2004**, *432*, 829−837.
(2) (a) Schreiber, S. L. *Science* **2000**, *287*, 1964−1969. (b) Burke, M. D.; Schreiber, S. L. *Angew. Chem., Int. Ed.* **2004**, *43*, 46−58.
(3) For chemical space, see: Dobson, C. M. *Nature* **2004**, *432*, 824−828.
(4) Zhang, L.; Carroll, P. J.; Meggers, E. *Org. Lett.* **2004**, *6*, 521−523.
(5) Bregman, H.; Williams, D. S.; Atilla, G. E.; Carroll, P. J.; Meggers, E. *J. Am. Chem. Soc.* **2004**, *126*, 13594−13595.
(6) Williams, D. S.; Atilla, G. E.; Bregman, H.; Arzoumanian, A.; Klein, P. S.; Meggers, E. *Angew. Chem., Int. Ed.* **2005**, *44*, 1984−1987.
(7) Metal-based drugs: (a) Orvig, C.; Abrams, M. J. (Eds.) *Chem. Rev.* **1999**, *99*, 2201−2842. (b) Guo, Z.; Sadler, P. J. *Angew. Chem., Int. Ed.* **1999**, *38*, 1512−1531. (c) Farrell, N. (Ed.) *Coord. Chem. Rev.* **2002**, *232*, 1−230.
(8) Metal complexes as enzyme inhibitors: Louie, A. Y.; Meade, T. J. *Chem. Rev.* **1999**, *99*, 2711−2734.
(9) For bioorganometallic chemistry, see: (a) Severin, K.; Bergs, R.; Beck, W. *Angew. Chem., Int. Ed.* **1998**, *37*, 1634−1654. (b) Grotjahn, D. B. *Coord. Chem. Rev.* **1999**, *190*, 1125−1141. (c) Jaouen, G. (Ed.) *J. Organomet. Chem.* **1999**, *589*, 1−126. (d) Metzler-Nolte, N. *Angew. Chem., Int. Ed.* **2001**, *40*, 1040−1043. (e) Fish, R. H.; Jaouen, G. *Organometallics* **2003**, *22*, 2166−2177. (f) Stodt, R.; Gencaslan, S.; Müller, I. M.; Sheldrick, W. S. *Eur. J. Inorg. Chem.* **2003**, 1873−1882. (g) Schlawe, D.; Majdalani, A.; Velcicky, J.; Hessler, E.; Wieder, T.; Prokop, A.; Schmalz, H.-G. *Angew. Chem., Int. Ed.* **2004**, *43*, 1731−1734. (h) Van Staveren, D. R.; Metzler-Nolte, N. *Chem. Rev.* **2004**, *104*, 5931−5985.
(10) For indolocarbazole protein kinase inhibitors, see: (a) Kase, H.; Iwahashi, K.; Nakanishi, S.; Matsuda, Y.; Yamada, K.; Takahashi, M.; Murakata, C.; Sato, A.; Kaneko, M. *Biochem. Biophys. Res. Commun.* **1987**, *142*, 436−440. (b) Ruegg, U. T.; Burgess, G. M. *Trends Pharmacol. Sci.* **1989** *10*, 218−220. (c) Martiny-Baron, G.; Kazanietz, M. G.; Mischak, H.; Blumberg, P. M.; Kochs, G.; Hug, H.; Marme, D.; Schachtele, C. *J. Biol. Chem.* **1993**, *268*, 9194−9197. (d) Caravatti, G.; Meyer, T.; Fredenhagen, A.; Trinks, U.; Mett, H.; Fabbro, D. *Bioorg. Med. Chem. Lett.* **1994**, *4*, 399−404. (e) Prudhomme, M. *Curr. Pharm. Des.* **1997**, *3*, 265−290. (f) Jackson, J. R.; Gilmartin, A.; Imburgia, C.; Winkler, J. D.; Marshall, L. A.; Roshak, A. *Cancer Res.* **2000**, *60*, 566. (g) Pindur, U.; Kim, Y. S.; Mehrabani, F. *Curr. Med. Chem.* **1999**, *6*, 29−69. (h) Zhu, G.; et al. *J. Med. Chem.* **2003**, *46*, 2027−2030.

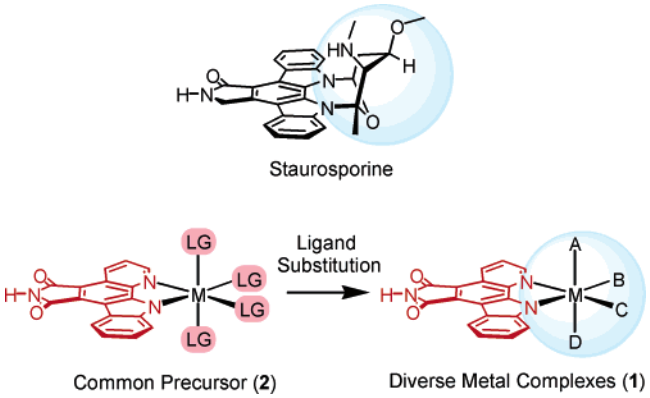

Figure 1. Mimicking the protein kinase inhibitor staurosporine with simple octahedral metal complexes. Indicated in blue are the globular domains of these compounds.

and hydrogen bonds within the globular ribose binding site. Thus, staurosporine matches the shape of the ATP binding site perfectly, which makes it a highly potent, albeit unspecific inhibitor for protein kinases. This distinctive globular three-dimensional structure of staurosporine is in contrast to many synthetic protein kinase inhibitors which mainly fill the adenine binding site with planar scaffolds and flexible side chains protruding into other regions of the active site.[12]

To match the shape of the ATP binding site of protein kinases in a fashion similar to staurosporine, but with less synthetic effort and more extended structural options, we replaced the indolocarbazole alkaloid scaffold with simple metal complexes in which the main features of the indolocarbazole aglycon are retained in the metal-chelating pyridocarbazole ligand (highlighted in red in Figure 1), thus targeting the metal complexes **1** to the ATP binding site (Figure 1). This places the metal center within the ribose binding site and gives the opportunity to build defined globular shapes by assembling ligands around the metal center. Following this strategy, we recently reported an organoruthenium half-sandwich scaffold for the highly potent inhibition of glycogen synthase kinase 3 (GSK3).[5,6]

To quickly scan for the most suitable ligand combination to fill up the coordination sphere around the ruthenium center, it would be desirable to have a compound which could serve as a common precursor for a large and diverse set of metal-containing compounds of type **1**. We here introduce such a metal complex **2** (Figure 1), which has four leaving groups in addition to the pyridocarbazole ligand, thus allowing for rapid access to a diversity of novel structures just by simple ligand replacement chemistry. On the basis of this concept, we report the discovery of inhibitors for the protein kinases MSK1, Pim1, and GSK3α.

Results and Discussion

As our common precursor **2**, we synthesized ruthenium complex **3**, bearing four leaving groups in addition to the pyridocarbazole ligand: three acetonitriles and one chloride (Figure 2).

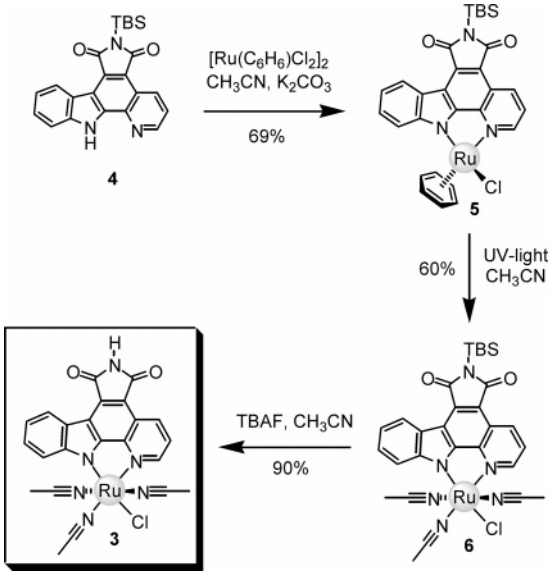

Figure 2. Synthesis of the precursor complex **3** for rapid ligand scanning.

Starting from the TBS-protected pyridocarbazole **4**, cyclometalation with $[(benzene)RuCl_2]_2$ at room temperature and in the presence of 1 equiv of K_2CO_3 yielded the half-sandwich complex **5** in 69% yield.[13] The benzene was subsequently replaced by three acetonitrile molecules upon photolysis with a medium pressure mercury lamp in acetonitrile, yielding complex **6** diastereoselectively in 60% yield.[14] Subsequent TBS deprotection with TBAF yielded the desired precursor complex **3**. A crystal structure of the N-benzylated derivative of **3** (Figure 3) reveals the stereochemistry with the chloride being *trans* to the indole nitrogen. It is worth noting that all three ruthenium complexes along this route (**5**, **6**, and **3**) are quite robust and are routinely purified with standard silica gel flash chromatography.

With precursor complex **3** in hand, we next investigated ligand substitution chemistry. The three acetonitrile ligands and the chloride do not undergo exchange reactions at room temperature, demonstrating the kinetical inertness of our pyridocarbazole−ruthenium scaffold. However, they can be replaced upon heating of **3** in the presence of ligands at elevated temperatures of 70−110 °C. For example, reaction of **3** with 2 equiv of 2,2′-bipyridine in ethanol at reflux for 1 h yields the complex **7** in 93% isolated yield after silica gel chromatography and precipitation as a hexafluorophosphate salt (Figure 4). Reaction of **3** with 1 equiv of 1,4,7-triazacyclononane provides in 74% yield the product **8**, in which two acetonitriles and the chloride are replaced by the tridentate ligand. Similarly, reaction of **3** with 1 equiv of 1,4,7-trithiacyclononane affords the analogous product **9** in 50% yield. The remaining acetonitrile ligand can subsequently be replaced with a variety of ligands, such as CO (**9**→**10**, 79%), cyanide (**9**→**11**, 15%), trimethyl phosphite (**9**→**12**, 60%), azide (**9**→**13**, 46% from in situ generated **9**), NH_3 (**9**→**14**, 41%), and DMSO (**9**→**15**, 65% from in situ generated **9**), among others. Figure 4 displays a representative set of metal complexes, which we synthesized

(11) For cocrystal structures of staurosporine with protein kinases, see for example: (a) Toledo, L. M.; Lydon, N. B. *Structure* **1997**, *5*, 1551−1556. (b) Lawrie, A. M.; Noble, M. E. M.; Tunnah, P.; Brown, N. R.; Johnson, L. N.; Endicott, J. A. *Nat. Struct. Biol.* **1997**, *4*, 796−801. (c) Prade, L.; Engh, R. A.; Girod, A.; Kinzel, V.; Huber, R.; Bossemeyer, D. *Structure* **1997**, *5*, 1627−1637.

(12) For protein kinase inhibitor scaffolds, see: (7) (a) García-Echeverría, C.; Traxler, P.; Evans, D. B. *Med. Res. Rev.* **2000**, *20*, 28−57. (b) Bridges, A. J. *Chem. Rev.* **2001**, *101*, 2541−2571.

(13) For the synthesis of pyridocarbazoles, see: Bregman, H.; Williams, D. S.; Meggers, E. *Synthesis* **2005**, 1521−1527.

(14) Adapted from: Gill, T. P.; Mann, K. R. *Organometallics* **1982**, *1*, 485−488. (b) Freedman, D. A.; Evju, J. K.; Pomije, M. K.; Mann, K. R. *Inorg. Chem.* **2001**, *40*, 5711−5715.

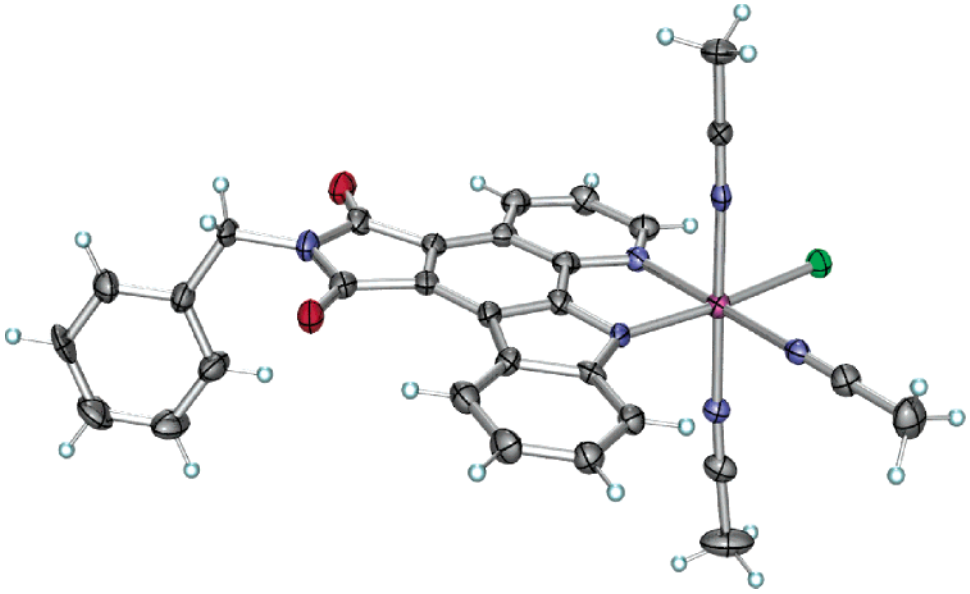

Figure 3. Crystal structure of the N-benzylated derivative of precursor complex **3**. ORTEP drawing with 40% probability thermal ellipsoids.

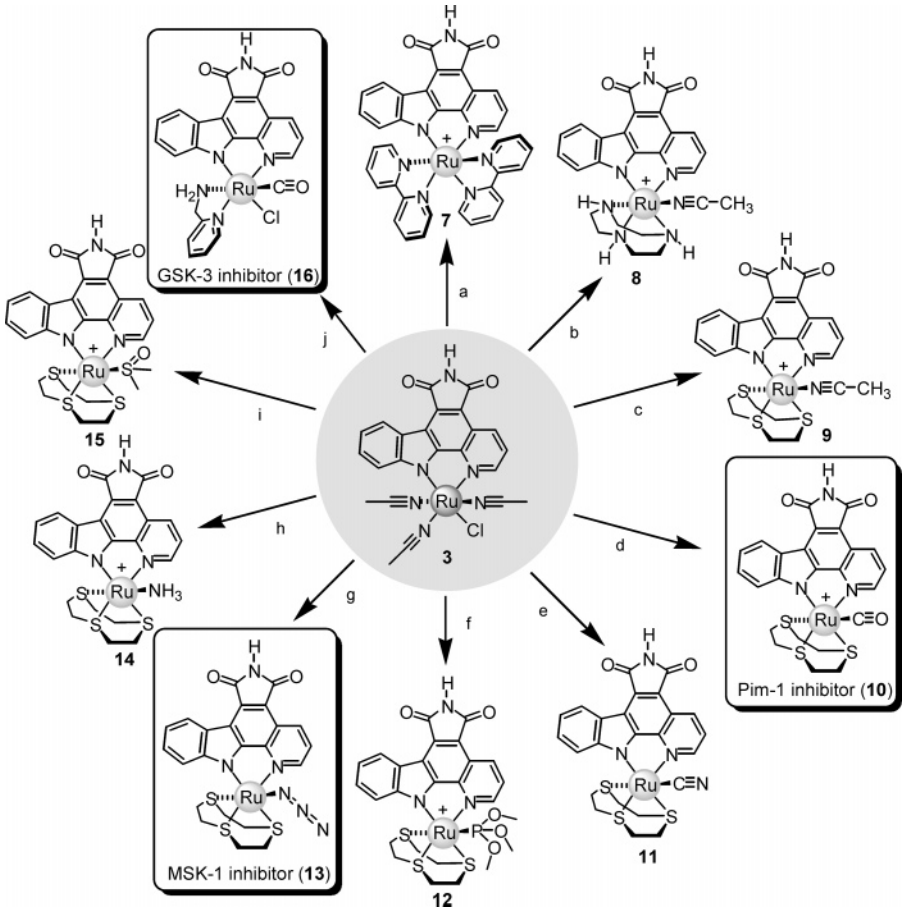

Figure 4. Ruthenium complex syntheses from precursor **3**. All cations were isolated as their PF_6 salts: (a) 2.2 equiv of 2,2′-bipyridine, EtOH, reflux, 1 h (93%); (b) 1.2 equiv of 1,4,7-triazacyclononane, reflux in EtOH for 2 h (65%); (c) 1.0 equiv of 1,4,7-trithiacyclononane, DMF, 80 °C for 45 min (50%). (d) From **9** by heating for 2 h in CO-saturated DMF to 95 °C (79%). (e) First, 1.0 equiv of 1,4,7-trithiacyclononane, DMF, 75 °C for 1 h, then addition of 1 equiv of NaCN and another hour at 90 °C (15%). (f) From **9** by heating with 2 equiv of $P(OMe)_3$ at 75 °C for 1 h (60%). (g) First, 1 equiv of 1,4,7-trithiacyclononane, DMF, 80 °C for 1 h, then addition of 1 equiv of NaN_3 and stirring at 90 °C for another hour (46%). (h) From **9** by heating in the presence of 0.17 M ammonia in DMF:dioxane (2:1) in a closed vessel for 1 h at 85 °C (41%). (i) First, 1.0 equiv of 1,4,7-trithiacyclononane, DMF, 85 °C for 1 h, then addition of 3.6 equiv of DMSO and stirring at 110 °C for another hour (65%). (j) First reaction in CO-saturated DMF at 75 °C for 1.5 h, then addition of 1 equiv of 2-aminomethylpyridine and heating for another 1.5 h at 95 °C (32%).

individually, isolated, and characterized spectroscopically. All shown compounds are racemates due to metal-centered chirality.

These examples demonstrate that we can use **3** as a precursor for synthesizing defined ligand spheres with mono-, bi-, and

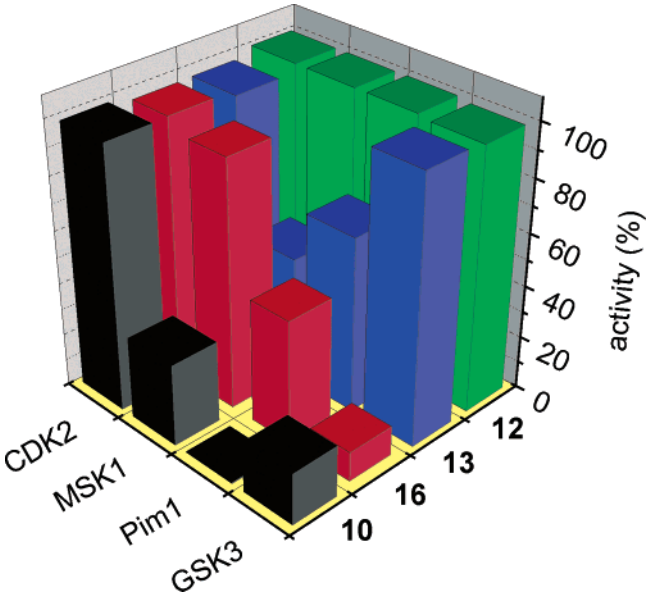

Figure 5. Activity of the organoruthenium compounds **10**, **12**, **13**, and **16** at a concentration of 100 nM against the protein kinases GSK3α, Pim1, MSK1, and CDK2/CyclinA. ATP concentration was 100 μM.

trivalent ligands, having a variety of coordinating functional groups, and adopting distinct three-dimensional globular shapes.

This method opens an avenue for the rapid scanning of ligands around the ruthenium center, searching for three-dimensional structures that are complementary in shape and functional group presentation to the active site of individual protein kinases. In fact, some of the compounds from Figure 4 were initially identified by screening of in situ synthesized libraries from precursor **3** and combinations of different ligands.[15] Figure 5 shows the activity of a set of selected compounds (**10**, **12**, **13**, and **16**) at a concentration of 100 nM against a small panel of the protein kinases CDK2/CyclinA,[16] MSK1,[17] Pim1,[18] and GSK3α.[19] For example, we identified the racemic compound **10** as a subnanomolar inhibitor for the protein kinase Pim1 (black bars in Figure 5). At 100 nM of **10**, the activity of Pim1 is reduced to less than 0.5%. Under the same conditions, the protein kinases GSK3α, MSK1, and CDK2/CyclinA still display activities of 19, 31, and 99%, respectively. The IC_{50} (concentration of compound at which 50% of the enzyme is inhibited) of **10** for Pim1 is 450 pM at 100 μM ATP and **10** is thus at least 2 orders of magnitude more potent against Pim1 than the unspecific inhibitor staurosporine (IC_{50} = 50 nM at 2 μM ATP; see Supporting Information). A Lineweaver−Burk kinetic analysis (Figure 6) confirms that **10** binds to Pim1 in an ATP

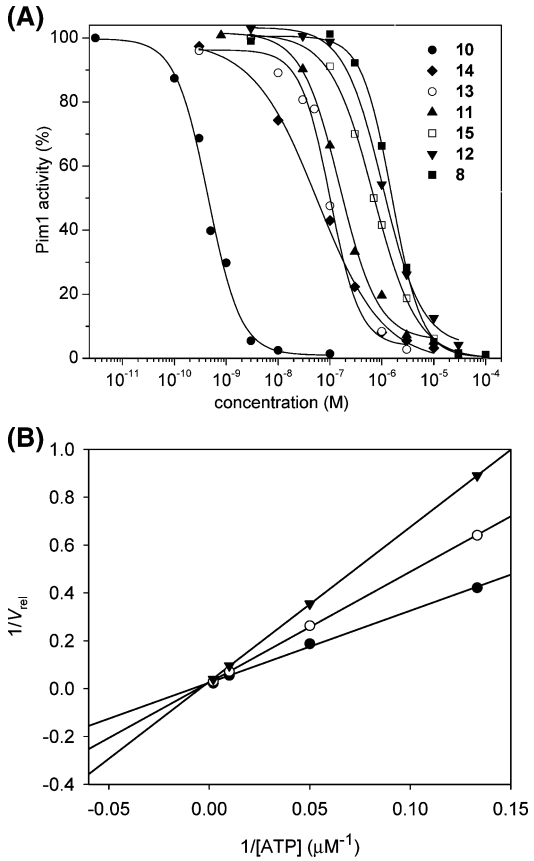

Figure 6. (A) IC_{50} curves with Pim1 obtained by phosphorylation of S6 kinase/Rsk2 Substrate Peptide 2 with [γ-^{32}P]ATP in the presence of 100 μM ATP and different concentrations of ruthenium complexes **8**, and **10**−**15**. (B) Double-reciprocal plots of relative initial velocities (V_{rel}) against varying ATP concentrations in the presence of 0 (●), 100 (○), and 200 pM (▼) of **10**.

competitive fashion. Curve fitting yields a remarkably low inhibition constant (K_i) of 90 ± 20 pM. In addition, methylation of the imide nitrogen of **10** reduces the activity by more than 2 orders of magnitude (IC_{50} = 120 nM at 2 μM ATP; see Supporting Information), reassuring that the imide N−H of **10** is involved in hydrogen bonding within the ATP binding site as designed.

To test the importance of the CO group in scaffold **10** for potency against Pim1, we synthesized compounds in which the CO group is exchanged for other monodentate ligands, such as cyanide (**11**), $P(OCH_3)_3$ (**12**), azide (**13**), NH_3 (**14**), and DMSO (**15**). This fast positional scanning would not be possible without the precursor complex **3**. It is noteworthy that, because of the cyclic nature of the tridentate ligand and the sp^3 hybridization at the coordinating sulfur atoms, 1,4,7-trithiacyclononane has to occupy both coordination sites within the plane of the pyridocarbazole ligand, thus leaving a position perpendicular to the pyridocarbazole plane for the coordination of a monodentate ligand (as an example, see Supporting Information for the crystal structure of N-benzylated **11**). This combination of a tridentate and monodentate ligand thus allows one to control the position of functional groups perpendicular to the plane of the pyridocarbazole ligand.

Intriguingly, all tested compounds are at least 2 orders of magnitudes less potent inhibitors for Pim1, as demonstrated by the IC_{50} curves shown in Figure 6. For example, replacing the CO group of **10** for a cyanide (**11**) reduces the IC_{50} for Pim1

(15) Small libraries with precursor **3** were typically prepared in 96-well plates by mixing **3** with different combinations of organic ligands in DMF and heating the solutions under air at 100 °C for 1−2 h. In the particular case of the discovery of **10** and **16**, we first introduced one CO ligand into **3** on a larger scale in a flask, then split the resulting solutions into 96-well plates, added additional ligands, and heated the solutions under air to 100 °C for 1.5 h. The resulting solutions were used without any further workup in screenings for protein kinase inhibition. See Supporting Information for an example.

(16) (a) Knockaert, M.; Greengard, P.; Meijer, L. *Trends Pharm. Sci.* **2002**, *23*, 417−425. (b) Huwe, A.; Mazitschek, R.; Giannis, A. *Angew. Chem., Int. Ed.* **2003**, *42*, 2122−2138.
(17) Deak, M.; Clifton, A. D.; Lucocq, J. M.; Alesi, D. R. *EMBO J.* **1998**, *17*, 4426−4441.
(18) Bachmann, M.; Möröy, T. *Int. J. Biochem. Cell Biol.* **2005**, 726−730.
(19) (a) Eldar-Finkelman, H. *Trends Mol. Med.* **2002**, *8*, 126−132. (b) Doble, B. W.; Woodgett, J. R. *J. Cell. Sci.* **2003**, *116*, 1175−1186. (c) Jope, R. S.; Johnson, G. V. W. *Trends Biochem. Sci.* **2004**, *29*, 95−102. (d) Cohen, P.; Goedert, M. *Nat. Rev. Drug Discovery* **2004**, *3*, 479−484.

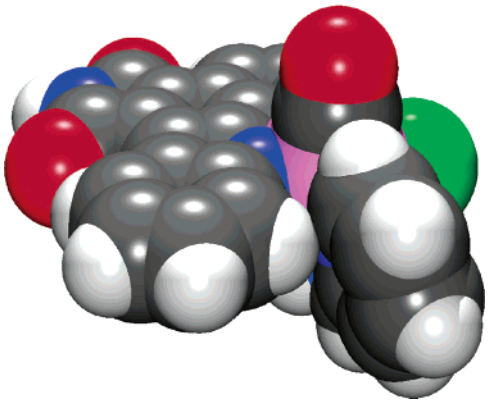

Figure 7. van der Waals space-filling representation of compound **16**. The coordinates are derived from a crystal structure of the N-benzylated derivative of **16** (see Supporting Information).

by a factor of 360 (IC_{50} = 160 nM). This is a remarkable modulation of activity by the change of just a single atom (including a change in overall charge). Similarly, exchanging the CO against azide (**13**) or NH_3 (**14**) reduces the activities by more than 2 orders of magnitude (IC_{50} = 100 and 80 nM, respectively), and replacing the CO against $P(OCH_3)_3$ (**12**) (IC_{50} = 800 nM) or DMSO (**15**) (IC_{50} = 1 μM) even leads to complexes that are more than a factor of 1000 less potent against Pim1. In fact, we even tested more monodentate ligands but did not find any ligand that can replace the CO group without significant reduction in affinity for Pim1 (data not shown). Interestingly, azide compound **13** is a quite potent inhibitor for the protein kinase MSK1 with an IC_{50} of 70 nM (see Figure 5).

After having discovered the opportunity to influence inhibitor selectivity by manipulating a single coordination site, we next turned our attention to the rest of the ligand sphere. The bar diagram in Figure 5 demonstrates that the CO compound **10** is most potent against Pim1, but also inhibits GSK3α to a significant extent at 100 nM (19% activity, IC_{50} = 14 nM at 100 μM ATP). Apparently, the CO ligand in the plane perpendicular to the pyridocarbazole chelate is an important pharmacophore both for Pim1 and GSK3, but not for most other kinases.[5,6] We were therefore wondering if we could now modulate the selectivity between the two kinases by the rest of the ligand sphere that complements the CO. Accordingly, scanning ligands starting again from precursor complex **3**, we discovered complex **16**, which differs from **10** by the replacement of the 1,4,7-trithiacyclononane ligand for an 2-aminomethylpyridine and chloride (Figure 4). The stereochemical identity of this compound was elucidated by X-ray crystal structure analysis of a benzylated derivative of **16** (see Supporting Information). Whereas **10** prefers Pim1 over GSK3α by a factor of 30 at 100 μM ATP, compound **16** displays selectivity for GSK3α, as visualized in the bar diagram of Figure 5. The IC_{50} of **16** for GSK3α is 8 nM at 100 μM ATP, and with this, **16** is by an order of magnitude more potent for GSK3α compared to Pim1 (IC_{50} = 95 nM).

The space-filling model of **16** (Figure 7) illustrates that the ruthenium center is buried and not accessible for direct interactions with the target protein. This is consistent with our model that the metal center has a solely structural role in organizing the orientation of the organic ligands and determining the overall shape of the molecule. In this regard, it is noteworthy that most of the discussed organometallic scaffolds are highly rigid. For example, ruthenium complex **16** cannot change its three-dimensional shape because of minimal rotational freedom. We assume that this rigidity plays an important role in generating highly selective protein kinase inhibitors because the molecule is not able to accommodate a different active site by adjusting the position of functional groups. We think that this hypothesis is manifested in the high selectivity of **16** for GSK3α. For example, **16** is significantly more potent for the α-isoform of GSK-3 (IC_{50} = 8 nM) over the β-isoform (IC_{50} = 50 nM). This is astonishing since GSK-3α and GSK-3β show 97% sequence identity within the ATP binding site.[20]

In conclusion, we here introduced a method which opens an avenue for the rapid scanning of ligands around a ruthenium center, searching for three-dimensional structures that are complementary in shape and functional group presentation to the active site of individual protein kinases. It is likely that inhibitor structures **10**, **13**, and **16** cannot be easily mimicked by an organic scaffold, and we believe that we are herewith accessing an area of the chemical space that is mostly unexplored.

Experimental Section

General Procedures and Reagents. NMR spectra were recorded on a Bruker AM-500 (500 MHz) or DMX-360 (360 MHz) spectrometer. Low-resolution mass spectra were obtained on an LC platform from Micromass using ESI technique. ES-TOF spectra were measured by Waters Micromass MS Technologies. High-resolution mass spectra were obtained with a Micromass AutoSpec instrument using either CI or ES ionization. Infrared spectra were recorded on a Perkin-Elmer 1600 series FTIR spectrometer. Solvents and reagents were used as supplied from Aldrich, Acros, or Strem. Reactions were performed under an atmosphere of argon unless otherwise specified. TBS-protected pyridocarbazole **4** was synthesized as published recently.[13] Protein kinases (human) and substrates were purchased from Upstate Biotechnology USA.

Compound 5. A suspension of **4** (1.84 g, 4.3 mmol), K_2CO_3 (654 mg, 4.73 mmol), and $[Ru(benzene)Cl_2]_2$ (1.1 g, 2.2 mmol) in CH_3CN (173 mL) was purged with argon and stirred overnight at ambient temperature. The resulting dark red suspension was dried in vacuo and the crude material subjected to silica gel chromatography with methylene chloride:methanol (first 100:1, then 20:1) as the eluting solvent. The product **5** was isolated as a red solid (1.84 g, 69%). ^{1}H NMR (500 MHz, $CDCl_3$): δ (ppm) 9.27 (d, J = 8.2 Hz, 1H), 9.19 (d, J = 4.6 Hz, 1H), 8.91 (d, J = 7.8 Hz, 1H), 7.83 (d, J = 8.1 Hz, 1H), 7.62−7.57 (m, 2H), 7.40 (t, J = 7.4 Hz, 1H), 5.94 (s, 6H), 1.04 (s, 9H), 0.62 (s, 3H), 0.61 (s, 3H). ^{13}C NMR (125 MHz, $CDCl_3$/CD_3OD): δ (ppm) 175.4, 174.8, 153.0, 151.7, 151.2, 142.6, 134.9, 132.6, 126.4, 125.1, 124.3, 122.8, 121.5, 119.9, 114.77, 114.74, 114.5, 83.4, 26.1, 18.8, −4.4. IR (film): ν (cm^{-1}) 3072, 2931, 2861, 1743, 1684, 1520, 1502, 1472, 1414, 1337, 1276, 1267, 1232, 1049, 826. HRMS calcd for $C_{31}H_{31}N_4O_2SiRu$ $(M - Cl + CH_3CN)^+$ 621.1260, found $(M - Cl + CH_3CN)^+$ 621.1276.

Compound 6. A suspension of **5** (235 mg, 0.38 mmol) was purged with argon for 15 min and then irradiated with a mercury medium pressure lamp (uranium filter) for 4 h while argon was bubbled through the solution. The resulting dark solution was dried in vacuo and the crude material subjected to silica gel chromatography with methylene chloride:methanol (20:1), yielding **6** (150 mg, 60%). Small quantities of a minor diastereoisomer were also isolated (17%). ^{1}H NMR (500 MHz, $CDCl_3$): δ (ppm) 9.61 (d, J = 4.1 Hz, 1H), 9.19 (d, J = 8.1 Hz, 1H), 8.93 (d, J = 8.0 Hz, 1H), 7.80 (br, 1H), 7.60 (dd, J = 8.4, 5.1

(20) Woodgett, J. R. *EMBO J.* **1990**, *9*, 2431−2438.

Hz, 1H), 7.55 (t, $J = 7.6$ Hz, 1H), 7.35 (br, 1H), 2.81 (s, 3H), 2.08 (s, 6H), 1.07 (s, 9H), 0.63 (s, 6H). IR (film): ν (cm^{-1}) 2928, 2855, 2326, 2271, 1748, 1684, 1579, 1520, 1415, 1347, 1319, 1292, 1269, 1228, 1132, 1046, 827, 749. HRMS calcd for $C_{29}H_{31}N_6O_2SiClRu$ $(M)^+$ 660.1010, found $(M)^+$ 660.1000.

Compound 3. To a stirred dark green solution of **6** (230 mg, 0.35 mmol) in CH_3CN (23 mL) was added tetrabutylammonium fluoride (523 μL, 1 M in THF, 0.522 mmol), and the solution was stirred at room temperature for 10 min. To the resulting dark pink solution was added glacial acetic acid (30 μL, 0.522 mmol), and it was stirred for 5 min, during which time a color change to green was observed. The solution was dried in vacuo and the resulting crude material subjected to silica gel chromatography with methylene chloride:methanol (20:1) to yield **3** (171 mg, 90%). ^{1}H NMR (500 MHz, $CDCl_3$): δ (ppm) 9.64 (d, $J = 4.0$ Hz, 1H), 9.14 (d, $J = 8.3$ Hz, 1H), 8.89 (d, $J = 7.9$ Hz, 1H), 7.81 (br, 1H), 7.63 (dd, $J = 8.3$, 5.1 Hz, 1H), 7.57 (t, $J = 7.7$ Hz, 1H), 7.39 (br, 2H), 2.82 (s, 3H), 2.05 (s, 6H). IR (film): ν (cm^{-1}) 2277, 1741, 1695, 1650, 1559, 1523, 1417, 1341, 1225, 1083, 1022, 951. HRMS calcd for $C_{23}H_{17}N_6O_2ClRu$ $(M)^+$ 546.0145, found $(M)^+$ 546.0170.

Compound 7. A suspension of **3** (10 mg, 0.018 mmol) and 2,2′-bipyridine (6.2 mg, 0.0396 mmol) in ethanol (1 mL) was purged with argon for 10 min and then refluxed for 1 h. The resulting brown suspension was dried in vacuo and the crude material subjected to silica gel chromatography with acetonitrile:water:saturated aqueous KNO_3 (50:3:1). The combined product eluents were concentrated to dryness, and the resulting material was dissolved in minimal acetonitrile/water. The product was precipitated by the addition of excess solid KPF_6. The precipitate was centrifuged and the pellet washed twice with water. The material was then dried under high vacuum to yield **7** (14.4 mg, 93%). ^{1}H NMR (500 MHz, acetone-d_6): δ (ppm) 9.85 (br, 1H), 9.11 (d, $J = 8.5$ Hz, 1H), 8.82−8.78 (m, 3H), 8.74 (d, $J = 8.1$ Hz, 1H), 8.68 (d, $J = 8.4$ Hz, 1H), 8.34 (d, $J = 5.1$ Hz, 1H), 8.26 (m, 2H), 8.18 (t, $J = 8.0$ Hz, 1H), 8.02 (m, 2H), 7.96 (t, $J = 8.6$ Hz, 1H), 7.93 (d, $J = 4.7$ Hz, 1H), 7.75 (d, $J = 4.8$ Hz, 1H), 7.64−7.60 (m, 3H), 7.32 (m, 2H), 7.20 (t, $J = 7.1$ Hz, 1H), 7.10 (t, $J = 6.9$ Hz, 1H), 5.92 (d, $J = 8.2$ Hz, 1H). ^{13}C NMR (125 MHz, DMSO-d_6): δ (ppm) 170.8, 170.7, 158.3, 158.2, 157.0 (higher intensity), 152.9, 152.2, 151.9, 151.5, 151.1, 151.0, 149.4, 143.1, 137.0, 136.9, 136.7, 136.5, 132.1, 130.5, 127.5, 127.4 (higher intensity), 127.4, 127.0, 126.0, 124.3, 124.1, 124.0, 123.9, 123.81, 123.77, 123.6, 121.1, 119.0, 115.0, 113.0, 112.9. IR (film): ν (cm^{-1}) 3178, 3131, 3060, 1749, 1696, 1578, 1525, 1461, 1420, 1343, 1261, 1226, 832, 767. HRMS calcd for $C_{37}H_{24}N_7O_2Ru$ $(M)^+$ 700.1035, found $(M)^+$ 700.1043.

Compound 8. A suspension of **3** (14.2 mg, 0.026 mmol) and 1,4,7-triazacyclononane (4 mg, 0.0312 mmol) in ethanol (1.4 mL) was purged with argon for 10 min and then refluxed for 2 h. The reaction mixture was cooled to room temperature, and diethyl ether (5 mL) was added to give a black precipitate. The precipitate was centrifuged and the pellet washed once with diethyl ether. The black solid obtained was further purified by filtration through Celite using methanol as the eluent, yielding **8** as its chloride salt (10 mg, 65%). ^{1}H NMR (360 MHz, CD_3-OD): δ (ppm) 9.15 (d, $J = 4.8$ Hz, 1H), 8.97 (d, $J = 8.3$ Hz, 1H), 8.75 (d, $J = 8.0$ Hz, 1H), 7.80 (d, $J = 8.2$ Hz, 1H), 7.61 (dd, $J = 8.3$, 5.1 Hz, 1H), 7.54 (t, $J = 7.6$ Hz, 1H), 7.28 (t, $J = 7.6$ Hz, 1H), 3.70−3.49 (m, 2H), 3.30−2.63 (m, 10H), 2.12 (s, 3H). IR (film): ν (cm^{-1}) 3371, 3260, 2962, 2919, 1693, 1586, 1416, 1343, 1258, 1228, 1083, 1028. HRMS calcd for $C_{25}H_{26}N_7O_2Ru$ $(M)^+$ 558.1191, found $(M)^+$ 558.1176.

Compound 9. To solution of **3** (29.3 mg, 0.054 mmol) in DMF (3 mL) was added 1,4,7-trithiacyclononane (536 μL, 100 mM in DMF). The solution was purged with argon for 5 min and then heated to 80 °C for 45 min. The resulting purple solution was dried in vacuo and coevaporated once with acetone. The crude material was subjected to silica gel chromatography with acetonitrile and later with acetonitrile:water:saturated aqueous KNO_3 (50:3:1). The combined product eluents were concentrated to dryness, and the resulting material was dissolved in minimal acetonitrile/water. The product was precipitated by the addition of excess solid NH_4PF_6. The precipitate was centrifuged and the pellet washed twice with water. The material was then dried under high vacuum to yield **9** (20 mg, 50%). ^{1}H NMR (360 MHz, acetone-d_6): δ (ppm) 9.94 (s, 1H), 9.30 (dd, $J = 8.4$, 1.2 Hz, 1H), 9.22 (dd, $J = 5.1$, 1.2 Hz, 1H), 8.91 (d, $J = 7.7$ Hz, 1H), 7.85 (m, 2H), 7.56 (t, $J = 7.7$ Hz, 1H), 7.37 (t, $J = 7.5$ Hz, 1H), 3.41−2.50 (m, 12H), 2.18 (s, 3H). ^{13}C NMR (75 MHz, acetone-d_6): δ (ppm) 171.2, 171.0, 155.0, 153.1, 152.2, 144.7, 134.9, 132.0, 127.1, 125.8, 125.6, 124.8, 124.3, 122.6, 120.1, 116.7, 115.6, 114.0, 35.5, 35.1, 34.8, 33.6, 33.5, 31.4, 3.4. IR (film): ν (cm^{-1}) 1753, 1702, 1523, 1490, 1417, 1343, 1228, 842, 750. HRMS calcd for $C_{25}H_{23}N_4S_3O_2Ru$ $(M)^+$ 609.0027, found $(M)^+$ 609.0032.

Compound 10. A solution of **9** (9 mg, 0.012 mmol) in DMF (2 mL) was purged with CO gas for 30 s, then stirred under an atmosphere of CO at 95 °C for 2 h. The resulting pink solution was dried in vacuo and coevaporated once with acetone. The crude material was subjected to silica gel chromatography with acetonitrile:water:saturated aqueous KNO_3 (50:3:1). The combined product eluents were concentrated to dryness, and the resulting material was dissolved in minimal acetonitrile/water. The product was precipitated by the addition of excess solid NH_4PF_6. The precipitate was centrifuged and the pellet washed twice with water. The material was then dried under high vacuum to yield **10** (7 mg, 79%). ^{1}H NMR (500 MHz, acetone-d_6): δ (ppm) 9.41 (dd, $J = 8.2$, 0.9 Hz, 1H), 9.17 (dd, $J = 5.1$, 1.0 Hz, 1H), 8.91 (d, $J = 8.3$ Hz, 1H), 7.96 (br s, 1H), 7.94 (dd, $J = 8.4$, 5.1 Hz, 1H), 7.74 (d, $J = 8.4$ Hz, 1H), 7.60 (t, $J = 7.6$ Hz, 1H), 7.41 (t, $J = 7.5$ Hz, 1H), 3.80−2.80 (m, 12H). ^{13}C NMR (75 MHz, DMSO-d_6): δ (ppm) (as acetate salt) 193.2, 173.6, 171.8, 171.4, 153.8, 153.6, 151.5, 143.3, 135.9, 131.8, 127.8, 125.6, 125.4, 124.8, 122.2, 120.6, 116.1, 115.1, 114.7, 38.9, 37.7, 36.8, 33.1, 32.4, 32.0, 23.8. IR (film): ν (cm^{-1}) 3389, 2014, 1702, 1584, 1414, 1343, 1226, 844. HRMS calcd for $C_{24}H_{20}N_3S_3O_3Ru$ $(M)^+$ 595.9710, found $(M)^+$ 595.9734.

Compound 11. To a solution of **3** (19.6 mg, 0.036 mmol) in DMF (1.15 mL) was added 1,4,7-trithiacyclononane (359 μL, 100 mM in DMF). The solution was purged with argon for 5 min and then heated to 75 °C for 1 h. To the resulting purple solution was added NaCN (359 μL, 100 mM in water). The reaction was stirred at 90 °C for 1 h, after which time the purple solution was dried in vacuo. The crude material was subjected to silica gel chromatography with methylene chloride:methanol (10:1), later changing to 5:1 and 3:1. The combined product eluents were dried to provide **11** (3.1 mg, 15%). ^{1}H NMR (500 MHz, DMSO-d_6): δ (ppm) 11.04 (s, 1H), 9.08 (dd, $J = 8.3$, 1.1 Hz, 1H), 8.96 (dd, $J = 5.0$, 1.1 Hz, 1H), 8.72 (d, $J = 7.8$ Hz, 1H), 7.74 (dd, $J = 8.4$, 5.1 Hz, 1H), 7.67 (d, $J = 8.4$ Hz, 1H), 7.50 (t, $J = 7.6$ Hz, 1H), 7.29 (t, $J = 7.4$ Hz, 1H), 3.10−2.23 (m, 12H). ^{13}C NMR (125 MHz, DMSO-d_6): δ (ppm) 171.0, 170.9, 153.4, 152.1, 150.4, 143.2, 139.8, 131.8, 130.2, 125.7, 124.1, 123.7, 123.3, 121.1, 118.8, 114.9, 114.5, 111.6, 36.2, 35.0, 33.5, 31.5, 30.3, 30.1. IR (film): ν (cm^{-1}) 2922, 2852, 2068, 1744, 1700, 1543, 1523, 1454, 1287, 1263, 1228, 668. HRMS (ESI-ToF) calcd for $C_{24}H_{21}N_4S_3O_2Ru$ $(MH)^+$ 594.9870, found $(MH)^+$ 594.9900.

Compound 12. To a solution of **9** (7 mg, 0.0093 mmol) in DMF (0.7 mL) was added trimethyl phosphite (2.2 μL, 0.0186 mmol) and heated to 75 °C for 1 h. The resulting purple solution was dried in vacuo and the crude material subjected to silica gel chromatography with acetonitrile and later acetonitrile:water:saturated aqueous KNO_3 (100:3:1). The combined product eluents were concentrated to dryness, and the resulting material was dissolved in minimal acetonitrile/water. The product was precipitated by the addition of excess solid NH_4PF_6. The precipitate was centrifuged and the pellet washed twice with water. The material was then dried under high vacuum to yield **12** (4.7 mg, 60%). ^{1}H NMR (500 MHz, CD_3CN): δ (ppm) 9.28 (d, $J = 8.3$ Hz, 1H), 8.89 (d, $J = 5.1$ Hz, 1H), 8.84 (d, $J = 7.8$ Hz, 1H), 8.72 (br, 1H), 7.74 (dd, $J = 8.4$, 5.1 Hz, 1H), 7.70 (d, $J = 8.2$ Hz, 1H), 7.60 (t, $J =$

7.6 Hz, 1H), 7.39 (t, $J = 7.4$ Hz, 1H), 3.30 (m, 1H), 3.13 (d, $J = 10.6$ Hz, 9H), 3.12−2.85 (m, 6H), 2.60−2.32 (m, 5H). ^{13}C NMR (90 MHz, CD_3CN): δ (ppm) 171.6, 171.3, 154.8, 153.3, 153.2, 144.9, 135.4, 132.5, 128.0, 126.2, 125.7, 124.9, 123.1, 121.1, 117.1, 116.0, 115.0, 54.1 (d, $J = 7.4$ Hz), 39.5 (d, $J = 8.5$ Hz), 38.1 (d, $J = 10.2$ Hz), 36.2, 32.5, 31.9 (d, $J = 2.3$ Hz), 30.9 (d, $J = 2.1$ Hz). IR (film): ν (cm^{-1}) 2944, 1751, 1702, 1521, 1491, 1418, 1344, 1227, 1045, 1016, 844, 746, 668, 638. HRMS calcd for $C_{26}H_{29}N_3PS_3O_5Ru$ $(M)^+$ 692.0050, found $(M)^+$ 692.0072.

Compound 13. To a solution of **3** (12.8 mg, 0.023 mmol) was added 1,4,7-trithiacyclononane (230 μL, 100 mM in DMF). The solution was purged with argon for 5 min and then heated to 80 °C for 1 h. To the resulting purple solution was added sodium azide (230 μL, 100 mM in water), and the solution was stirred for 1 h at 90 °C. The resulting purple solution was dried in vacuo and subjected to silica gel chromatography with methylene chloride:methanol 20:1 and later 10:1 to provide **13** (6.6 mg, 46%). ^{1}H NMR (500 MHz, DMSO-d_6): δ (ppm) 10.99 (s, 1H), 9.09 (dd, $J = 8.3$, 1.1 Hz, 1H), 9.07 (dd, $J = 5.1$, 1.2 Hz, 1H), 8.73 (d, $J = 7.8$ Hz, 1H), 7.77 (m, 2H), 7.50 (t, $J = 7.6$ Hz, 1H), 7.29 (t, $J = 7.5$ Hz, 1H), 3.07−2.19 (m, 12H). ^{13}C NMR (90 MHz, DMSO-d_6): δ (ppm) 171.0, 170.9, 153.9, 152.1, 150.5, 143.4, 132.2, 130.2, 125.7, 124.1, 123.8, 123.3, 121.1, 118.7, 115.0, 114.7, 111.7, 34.6, 33.9, 33.4, 32.6, 31.7, 29.4. IR (film): ν (cm^{-1}) 2026 (N_3), 1740, 1697, 1658, 1562, 1519, 1415, 1337, 1285, 1229, 1129, 934, 873, 752, 696, 678. ES-ToF $(M - H)^-$ 609.0.

Compound 14. To a solution of **9** (10 mg, 0.013 mmol) in DMF (1 mL) was added ammonia (0.5 M in dioxane) (500 μL, 0.25 mmol). The reaction vessel was closed with a septum and heated to 85 °C for 1 h, and the purple solution was dried in vacuo. The crude material was subjected to silica gel chromatography with acetonitrile:water: saturated aqueous KNO_3 100:3:1, later changing to 50:3:1. The combined product eluents were concentrated to dryness, and the resulting material was dissolved in minimal acetonitrile/water. The product was precipitated by the addition of excess solid NH_4PF_6. The precipitate was centrifuged and the pellet washed twice with water. The material was then dried under high vacuum to yield **14** (4 mg, 41%). ^{1}H NMR (360 MHz, DMSO-d_6): δ (ppm) 11.03 (br s, 1H), 9.12 (d, $J = 8.3$ Hz, 1H), 9.04 (d, $J = 5.0$ Hz, 1H), 8.74 (d, $J = 7.8$ Hz, 1H), 7.78 (dd, $J = 8.4$, 5.1 Hz, 1H), 7.74 (d, $J = 8.6$ Hz, 1H), 7.52 (t, $J = 7.6$ Hz, 1H), 7.30 (t, $J = 7.3$ Hz, 1H), 3.01−2.06 (m, 15H). ^{13}C NMR (90 MHz, DMSO-d_6): δ (ppm) 171.0, 170.9, 153.9, 152.1, 151.5, 143.3, 132.7, 130.2, 125.8, 124.2, 124.0, 123.5, 121.2, 118.9, 114.95, 114.93, 112.2, 34.3, 33.3, 33.1, 32.9, 31.7, 30.2. IR (film): ν (cm^{-1}) 3317, 3238, 2924, 2845, 1690, 1646, 1587, 1523, 1489, 1415, 1341, 1287, 1223, 1150, 1130, 1080, 1022, 1007, 845, 742, 707, 643, 560. HRMS calcd for $C_{23}H_{23}N_4S_3O_2Ru$ $(M)^+$ 585.0027, found $(M)^+$ 585.0055.

Compound 15. To a solution of **3** (17 mg, 0.031 mmol) was added 1,4,7-trithiacyclononane (310 μL, 100 mM in DMF). The solution was purged with argon for 5 min and then heated to 85 °C for 1 h. To the resulting purple solution was added dimethyl sulfoxide (80 μL, 1.13 mmol), stirred for 1 h at 110 °C, and thereafter dried in vacuo. The material was coevaporated with ethanol and then subjected to silica gel chromatography with acetonitrile:water:saturated aqueous KNO_3 (50:3:1). The combined product eluents were concentrated to dryness, and the resulting material was dissolved in minimal acetonitrile/water. The product was precipitated by the addition of excess solid KPF_6. The precipitate was centrifuged and the pellet washed twice with water. The material was then dried under high vacuum to yield **15** (16 mg, 65%). ^{1}H NMR (500 MHz, acetone-d_6): δ (ppm) 9.97 (s, 1H), 9.36 (m, 2H), 8.92 (d, $J = 8.0$ Hz, 1H), 7.95 (dd, $J = 8.3$, 5.1 Hz, 1H), 7.87 (d, $J = 8.2$ Hz, 1H), 7.64 (t, $J = 7.6$ Hz, 1H), 7.41 (t, $J = 7.5$ Hz, 1H), 3.50−2.93 (m, 12H), 2.57 (s, 3H), 2.54 (s, 3H). ^{13}C NMR (125 MHz, DMSO-d_6): δ (ppm) 171.1, 170.8, 154.2, 153.3, 152.2, 144.3, 135.9, 132.2, 128.0, 126.3, 125.9, 125.2, 123.1, 120.9, 117.3, 115.2, 115.1, 46.1, 44.4, 36.1, 35.9, 34.9, 32.9 (higher intensity), 32.5. IR (film): ν (cm^{-1}) 1745, 1694, 1621, 1484, 1411, 1342, 1224, 1077, 1013, 840, 748. HRMS calcd for $C_{25}H_{26}N_3S_4O_3Ru$ $(M)^+$ 645.9901, found $(M)^+$ 645.9870.

Compound 16. A solution of **3** (40 mg, 0.073 mmol) in DMF (4 mL) was purged with CO gas for 30 s then heated under an atmosphere of CO at 75 °C for 1.5 h. A color change from green to pink was observed. To the solution was added 2-aminomethylpyridine (7.6 μL, 0.073 mmol), and the resulting solution was heated to 95 °C for 1.5 h. The resulting purple solution was dried in vacuo and coevaporated with ethanol. The crude material was subjected to silica gel chromatography with methylene chloride:methanol 50:1, and later with 35:1, yielding **16** (13 mg, 32%), in addition to 32% of a diastereomeric product. ^{1}H NMR (500 MHz, acetone-d_6): δ (ppm) 9.82 (br, 1H), 9.38 (d, $J = 5.5$ Hz, 1H), 9.34 (dd, $J = 5.1$, 1.2 Hz, 1H), 9.23 (dd, $J = 8.4$, 1.3 Hz, 1H), 8.77 (ddd, $J = 7.9$, 1.3, 0.7 Hz, 1H), 8.07 (td, $J = 7.8$, 1.5 Hz, 1H), 7.85 (dd, $J = 8.4$, 5.1 Hz, 1H), 7.67 (m, 2H), 7.21 (ddd, $J = 7.8$, 7.0, 0.9 Hz, 1H), 7.16 (ddd, $J = 8.3$, 7.0, 1.4 Hz, 1H), 6.11 (d, $J = 8.1$ Hz, 1H), 4.88 (m, 1H), 4.76 (m, 2H), 4.21 (m, 1H). ^{13}C NMR (90 MHz, DMSO-d_6): δ (ppm) 200.4, 171.0, 170.7, 164.6, 155.7, 154.3, 151.2, 151.1, 144.1, 137.8, 133.1, 130.4, 125.9, 124.6, 124.1, 123.4, 122.8, 121.8, 120.8, 118.9, 114.4, 112.9, 112.8, 49.2. IR (film): ν (cm^{-1}) 3216, 2925, 1944, 1749, 1699, 1581, 1526, 1494, 1476, 1421, 1344, 1226, 1130, 1017. HRMS (ESI-ToF) calcd for $C_{24}H_{15}N_5O_3ClRu$ $(M - H)^-$ 557.9907, found $(M - H)^-$ 557.9916.

Protein Kinase Assays. Various concentrations of inhibitors were incubated at room temperature in 20 mM MOPS, 30 mM $MgCl_2$, 0.8 μg/μL BSA, 5% DMSO (resulting from the inhibitor stock solution), pH 7.0, in the presence of substrate (Pim1 = 50 μM S6 kinase/Rsk2 Substrate Peptide 2; MSK1 = 30 μM crosstide; GSK3α = 20 μM phosphoglycogen synthase peptide-2; CDK2/CyclinA = 0.1 μg/μL histone H1) and kinase (Pim1 = 0.02 ng/μL for IC_{50} determinations and 0.4 ng/μL for the determination of activities at 100 nM inhibitor concentration (bar diagram in Figure 4); MSK1 = 0.4 ng/μL; GSK3α = 0.4 ng/μL; Cdk2/CyclinA = 0.8 ng/μL). After 15 min, the reaction was initiated by adding ATP to a final concentration of 100 μM, including approximately 0.2 μCi/μL [γ-^{32}P]ATP. Reactions were performed in a total volume of 25 μL. After 30 min, the reaction was terminated by spotting 17.5 μL on a circular P81 phosphocellulose paper (diameter = 2.1 cm, Whatman), followed by washing four times (5 min each wash) with 0.75% phosphoric acid and once with acetone. The dried P81 papers were transferred to a scintillation vial, and 5 mL of scintillation cocktail was added, and the counts per minute (CPM) were determined with a Beckmann 6000 scintillation counter. IC_{50} values were defined to be the concentration of inhibitor at which the CPM was 50% of the control sample, corrected by the background.

Lineweaver−Burk Kinetics. Various concentrations of ATP and inhibitor **10** were incubated at room temperature for 1 h in 20 mM MOPS, 30 mM $MgCl_2$, 0.8 μg/μL BSA, 5% DMSO (resulting from the inhibitor stock solution), pH 7.0, in the presence of S6 kinase/ Rsk2 Substrate Peptide 2 (50 μM) and Pim1 (human, 0.022 ng/μL). The total reaction volume was 25 μL. Each ATP solution contained the same ratio of ATP to radioactive [γ-^{32}P]ATP and were as follows: 500 μM ATP with 0.40 μCi/μL [γ-^{32}P]ATP, 100 μM ATP with 0.08 μCi/μL [γ-^{32}P]ATP, 20 μM ATP with 16 nCi/μL [γ-^{32}P]ATP, and 4 μM ATP with 3.2 nCi/μL [γ-^{32}P]ATP. The inhibitor concentrations used were 0, 0.1, 0.2, 0.5, and 1 nM. Prior to the addition of ATP, the inhibitor **10**, substrate, and protein kinase were preincubated for 20 min in the reaction buffer. After 1 h, the reactions were stopped by spotting 17.5 μL of the reaction solution on a circular P81 phosphocellulose paper (diameter = 2.1 cm, Whatman) followed by washing four times (5 min each wash) with 0.75% phosphoric acid and once with acetone. After the papers dried, they were transferred to scintillation vials, and 5 mL of scintillation cocktail was added. The counts per minute (CPM) were measured with a Beckmann 6000 scintillation

counter. CPM values were treated as relative initial velocities. All reactions were performed at least in duplicate. The inhibition constant (K_i) of **10** was calculated by nonlinear regression using the software GraphPad Prism (version 4.0).

Acknowledgment. We thank the University of Pennsylvania and the National Institutes of Health (1 R01 GM071695-01A1) for financial support of this research.

Supporting Information Available: IC_{50} curves, crystallographic data, ^1H NMR spectrum of precursor **3**, an example of the synthesis of an in situ ruthenium complex library, and complete ref 10h. This material is available free of charge via the Internet at http://pubs.acs.org.

JA055523R